Triggering Cu-coordination change in Cu(ii)-Ala-His-His by external ligands

Paulina Gonzalez, Karolina Bossak-Ahmad, Bertrand Vileno, Nina E Wezynfeld, Youssef El Khoury, Petra Hellwig, Christelle Hureau, Wojciech Bal, Peter Faller

Triggering Cu-coordination change in Cu(II)-Ala-His-His by external ligands

Paulina Gonzalez [#,1, 2, 3], Karolina Bossak-Ahmad [#,4], Bertrand Vileno [1,5], Nina E. Wezynfeld[1], Youssef El Khoury [6], Petra Hellwig [2,6], Christelle Hureau [2,3*], Wojciech Bal [4*], Peter Faller [1, 2*]

[1] Institut de Chimie, UMR 7177, CNRS-Université de Strasbourg, 4 rue Blaise Pascal, 67000, Strasbourg, France.

[2] University of Strasbourg Institute for Advanced Study (USIAS), Strasbourg, France

[3] LCC-CNRS, Université de Toulouse, CNRS, Toulouse, France

[4] Institute of Biochemistry and Biophysics, Polish Academy of Sciences, Pawińskiego 5a, 02-106 Warsaw, Poland.

[5] French EPR Federation of Research (REseau NAtional de Rpe interDisciplinaire (RENARD), Fédération IR-RPE CNRS #3443), France.

[6] Laboratoire de Bioélectrochimie et Spectroscopie, UMR 7140, Université de Strasbourg, 4 Rue Blaise Pascal, 67000, Strasbourg, France

* : corresponding authors

# Contributed equally to the work

Cu(II) forms well-known and stable complexes with peptides having histidine at position 2 (Xxx-His) or 3 (Xxx-Zzz-His). Their properties differ considerably due to the histidine positioning. Here we report that in the hybrid motif Xxx-His-His, the Cu(II)-complexes can be switched between the Xxx-His and the Xxx-Zzz-His coordination modes by addition of external ligands.

Cu is an essential element for most of the living organisms, however, it can also be potentially dangerous. Therefore, most of Cu is bound to biomolecules, mainly to proteins with some contribution from peptides. This allows the control of its chemistry via the coordination sites.[1–6] Among many coordination modes identified in copper biochemistry, two are very characteristic due to their minimal sequence requirements. They consist of only two or three amino acids at the N-terminus (with a free amine), i.e. the NH_2-Xxx-His (XH) and NH_2-Xxx-Zzz-His (XZH) sequences, where Zzz are any amino acids but Pro. The best known representatives of these motifs are the tripeptide GHK, and the N-terminal sequence DAHK of the human serum albumin (HSA).[1,7] GHK possesses a variety of Cu-dependent biological activities, such as acceleration of wound healing and tissue remodeling.[8] HSA is a well-established Cu carrier in the blood. These sites are specific for Cu(II) ions over the other essential metal ions in humans and the respective complexes have been thoroughly described (Scheme 1).[7,9–13] The XH sequence provides a planar arrangement of three equatorial ligands around the Cu(II) ion with the NH_2 of the N-terminus, the N_π of the imidazole of His and the nitrogen of the peptide bond between X and H (NH_2, N, N^{Im}; called 3N). An external ligand (L) completes this coordination sphere forming 3N+L complexes (in simple model systems L often includes water). XZH binds Cu(II) with the NH_2, $2N^-$, N^{Im} set, called 4N (Scheme 1). This motif comprises one more peptide bond nitrogen and hence the equatorial coordination plane is complete.

Despite their partial resemblance in coordination, Cu(XZH) and Cu(XH) complexes differ in many aspects. This includes their spectroscopic properties, correlated with one different donor atom.[14,15] The time scales of Cu(II) self-exchange reactions are dramatically different: they are slow for XZH (minutes) but fast for XH (< seconds).[16] With respect to redox properties, Cu(II) coordinated to XZH can be oxidized to Cu(III) while Cu(II) in a Cu(XH) complex can be reduced to Cu(I) in the [-1.0,+1.0 V/vs SCE range].[11] Nevertheless, their thermodynamic stability around pH 7.4 is often within the same order of magnitude, with dissociation constants lower than pM.[17]

We previously investigated the Cu(II) complexes of Ala-His-His-OH (AHH) and Ala-His-His-NH_2 (AHH-am) peptides, chimeras of these two motifs, and demonstrated that they actuate the 3N and the 4N binding modes reversibly as a function of pH.[15] The same modes were also described beforehand by Jackson et al. for the peptide sarcosyl-His-His, which has a secondary amine instead of the primary one at the N-terminus.[18] Taking advantage of the labile equatorial site in the 3N coordination mode, the present work explores the ability of external, nitrogen bearing ligands L to switch between the 3N+L and 4N binding modes in the Cu(AHH) system for L

including imidazole and azide, seeking their effect on Cu(II) reactivity in the biotechnological and biochemical context.

As we demonstrated previously, in AHH at pH 7.4 Cu(II) is predominantly (~90%) bound in the 4N form with a typical absorption maximum of the *d-d* band at ~520 nm. The 3N+L form with a water molecule as L was only predominant at pH below 5.5.[15]


"4N form"   **"3N + L form"**
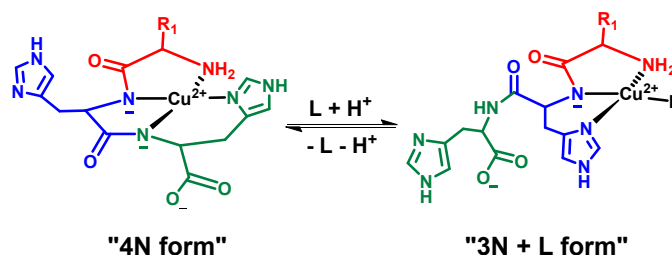
Scheme 1: Peptides with the sequence Xxx-His-His contain the two motifs XZH and XH . Therefore, Cu(II) can bind to either motif, i.e. with the coordination sphere NH_2, $2N^-$, N^{Im} (4N) or NH_2, N^-,N^{Im}, L, (3N+L) where L stands for external ligand. The equilibrium is dependent on pH, type and concentration of L. R1 is the present case is Ala, but can be another amino acid.

In order to see if the Cu(II)-coordination can be pushed from the 4N to the 3N+L form, at the physiologically relevant pH value of 7.4, we added external ligands that could substitute the water molecule bound to the 3N form and therefore stabilize it. The external ligand chosen was imidazole (Im) as a mimic of the side chain of the His residue, the main metal binding site in proteins. Imidazole is also a relatively strong ternary ligand for XH peptides, as demonstrated recently.[12,19] In these experiments AAH and AH peptides were used as references representing pure 4N and 3N coordination modes, respectively.
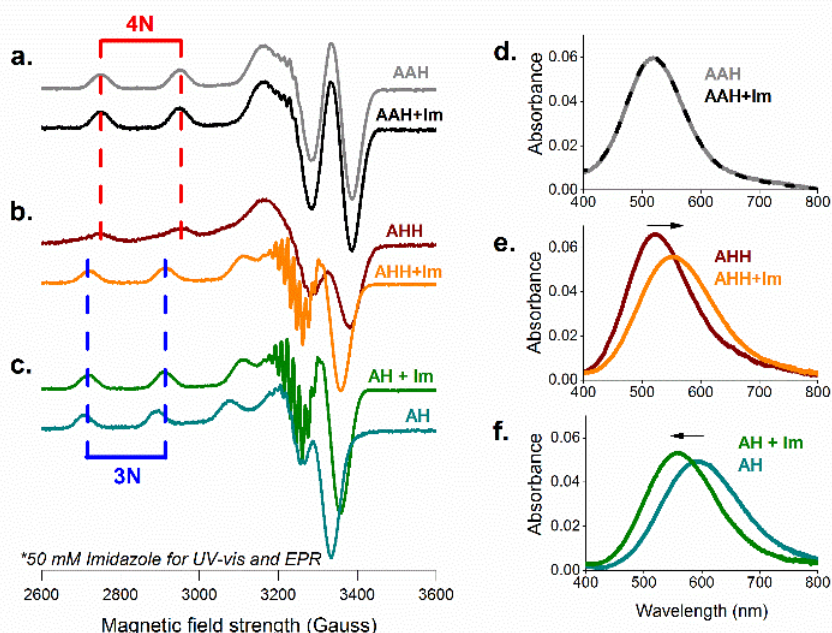
Figure 1: EPR spectra of a) Cu(AAH), b) Cu(AHH), and c) Cu(AH) with and without Im (50 mM) at pH 7.4. Experimental conditions: 1.6 mM $CuCl_2$, 2 mM peptide, 100 mM HEPES buffer, pH 7.4, 30% glycerol at 100 K. Dotted lines indicate the lowest field peak of the Cu(II) parallel hyperfine splitting constant of the 3N+N^{Im} (blue) and 4N (red) complexes, respectively. UV-Vis spectra of Im titrations of d) Cu(AAH), e) Cu(AHH) and f) Cu(AH). Experimental conditions: 0.8 mM $CuCl_2$, 1 mM peptide, 0 mM or 50 mM Im, at room temperature and pH 7.4, controlled manually. Black arrows indicate the direction of changes upon Im addition.

In the absence of Im, Cu(AHH) shows an absorption band with λ_{max} at 522 nm, in line with the predominant presence (~89%) of the 4N form, (Fig. 1e, brown) (The remaining 11% comprises the 3N form (7%) and the auto-ternary 3N+N^{His} complex (4%). For spectroscopic parameters see Table S1. Upon stepwise Im additions the band redshifts until the saturation at around 200 mM of Im (λ_{max} = 560 nm, ϵ =68 L mol^{-1} cm^{-1}) (Fig. 1e, orange). The final band's maximum corresponds to the formation of a ternary Cu(II)-complex where the 3N chelating unit of the peptide AHH was complemented by the external Im (3N+N^{Im}).[11] The observed red-shift is consistent with the replacement in the copper coordination sphere, where one amide nitrogen is being substituted with a nitrogen from the external Im[10,13,20,21] (Fig. 1). Similarly, we monitored the 3N+N^{Im} complex formation via CD spectroscopy. The data are in agreement with the UV-vis spectroscopy. Cu(AHH) exhibited the spectrum typical for 4N complexes with the asymmetrically split *d-d* band (458 nm and 543 nm for the maximum and minimum) and charge transfer (CT) bands at 273 and 313 nm. The addition of Im at pH 7.4 changed the spectral pattern substantially, in line with the spectra of pure 3N+N^{Im} complexes. This pattern is dominated by a positive *d-d* band at 556 nm (See Fig. S1). These results are corroborated by EPR spectra of Cu(AHH) (Fig. 1a-c, S2, Table S1 & 2). In the absence of Im (Fig. 1b, brown) the complex is mainly in the 4N form. The parameters g$_{//}$ = 2.18(2) and A$_{//}$ 614 MHz are typical for 4N Cu(XZH) complexes, including Cu(AAH) (Fig. 1; Table S1 & 2 for EPR parameters).[15] The addition of Im (Fig. 1b, orange) yielded a spectrum with g$_{//}$ = 2.21(1) and A$_{//}$ 596 MHz, very similar to that of the canonical Cu(GHK) ternary complex with Im[11], matching the formation of the 3N+N^{Im} complex (for AH see Fig. 1c, green and Table S1 & 2).[11] All Cu(II) complexes observed lie in a square planar geometry as deduced from the g$_{//}$/A$_{//}$ value (Tables S1 and S2). In addition, the very same behaviour in EPR were observed when N-methyl-imidazole instead of Im was used in line with monodentate coordination of neutral Im (Fig. S2). Therefore, UV-vis, CD and EPR spectroscopies indicate that addition of the external ligand Im can shift the Cu(II)-coordination from the 4N to the 3N + N^{Im} type with Im in its neutral form. The concentration dependences of changes in *d-d* bands of Cu(AAH) and Cu(AH) induced by Im are shown in Fig. 2. The apparent binding constant for Cu(AHH)(Im) calculated from these titration, $^cK_{7.4}$ = 111±4 M^{-1}.
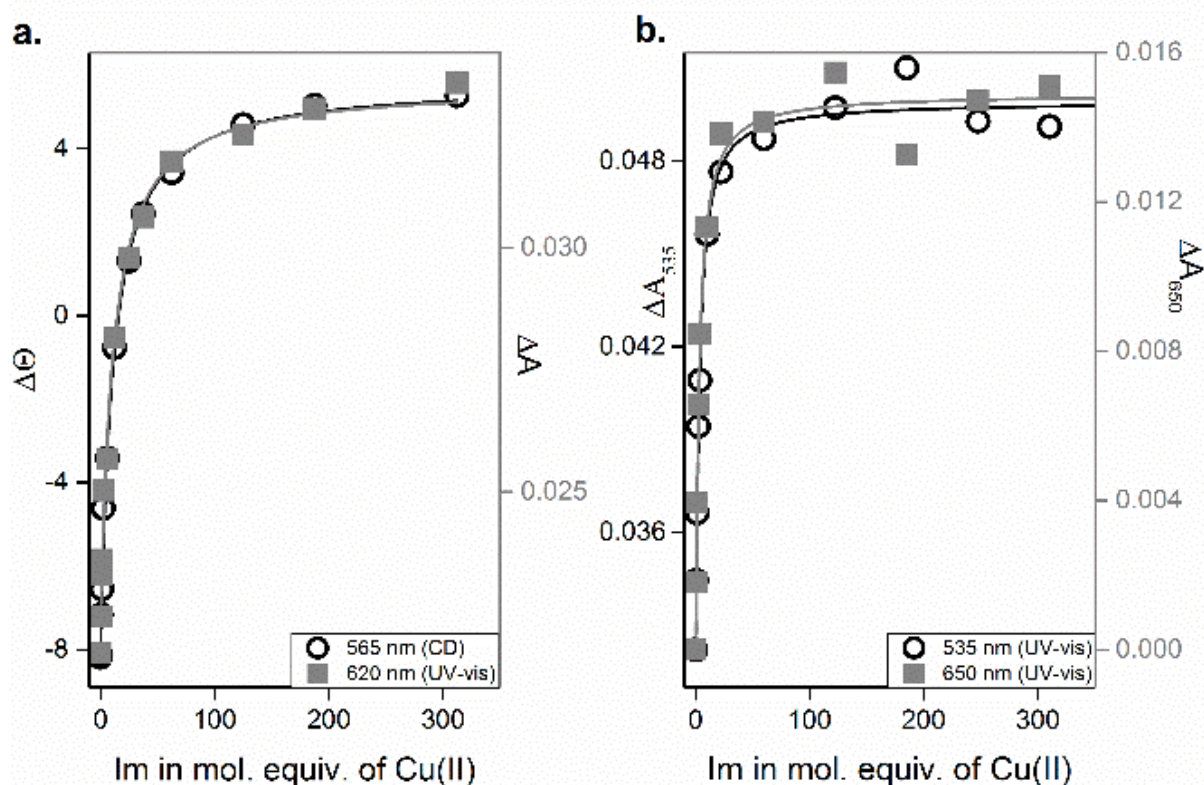

Figure 2: Dependence of absorption and ellipticity changes on proportion of Im to copper complexes of a) AHH and b) AH. Experimental conditions: 1 mM peptide, 0.8 mM CuCl$_2$ titrated with up to 300 mM Im, pH 7.4. Solid lines represent global fitting of data at different wavelengths for each peptide.

The interaction of Im with Cu(AH) yielded a blue shift of the *d-d* band to 560 nm, completed at around 50 mM of Im. This blue-shift correlates with the replacement of the coordinated H_2O oxygen by an Im nitrogen (Fig. 1f, green).[13] The resulting band is very similar to that for Cu(AHH) with Im in terms of spectral parameters e.g. ε = 68 L mol^{-1} cm^{-1}, the same as for Cu(AH)). It is well established in the literature that other Cu(XH)(Im) complexes have *d-d* bands around 560 nm.[11,16,22] These results are also confirmed by EPR spectroscopy where the addition of Im to Cu(AH) yielded a change of $g_\parallel$ (Fig. 1c, green, Table S1) which matches the shift from a 3N to a 3N + N^{Im} form.[11,22,23] Moreover, in the region of $g_\perp$ the addition of Im induced a well resolved superhyperfine interaction, which is clearly different from that in the Cu(Im)$_x$ sample (Fig. S2), supporting the inability of Im to withdraw Cu(II) from the studied peptides. The $^cK_{7.4}$ = 434±14 M^{-1} for the Im binding to Cu(AH) was four times higher than the apparent value obtained for Cu(AHH) (Table S3). This can be explained by a strong competition between 4N and 3N+N^{Im} in Cu(AHH) where only 7% of copper at pH 7.4 is bound in the 3N complex. Therefore the mechanism of ternary complex formation is different: for Cu(AH) the fourth binding site is occupied by a labile water molecule, thus easily accessible for external ligand, whereas in Cu(AHH) the 4N Cu(II) binding site needs to be internally rearranged, to be followed by ternary complex formation.

We also titrated Im under the same condition to Cu(AAH) as a negative control. This complex exhibited the λ$_{max}$ value of about 518 nm, typical for the 4N motif (Fig. 1d, grey). No shift of the band was observed up to 200 mM Im (Fig. 1d, navy), consistent with the absence of Im binding due to the saturated equatorial coordination sphere of Cu(AAH). The EPR spectrum of Cu(AAH) also did not change after Im addition, confirming the absence of Im binding (Fig. 1a, grey and navy). All spectra for titrations of Cu(AHH), Cu(AH) and Cu(AAH) with Im are shown in Fig. S3.

Knowing that the Im addition can shift the coordination mode from 4N to 3N+N^{Im}, we investigated further the Cu(AHH)(Im) complex formation *via* potentiometry, complemented by UV-Vis and CD spectroscopic titrations (Fig. 3 and S4). AHH protonation constants and Cu(AHH) stability constants obtained by potentiometry were reported previously and were used for calculation of Cu(AHH)(Im) stability constants (see Table 1 for the full potentiometric model).

In the UV-Vis spectra (Fig. 3a) of Cu(II)/AHH (=L in the next paragraph)/Im titrated with NaOH in the pH range 2.5-12, the aqua-Cu(II) band (λ$_{max}$ = 816 nm), visible at low pH, decreased rapidly above pH 2.5, becoming a minor species already at pH 3.5. This is due to the early formation of monodentate Cu(Im) complex that gives rise to a weak absorption band around 750 nm. Later, almost simultaneously CuHL, Cu(Im)$_2$ and CuL complexes are formed with the maximal appearance at pH 3.9, 4.15 and 4.6, respectively (see Fig. 2b). The peptide complexes are confirmed by CD spectroscopy (See Fig. S4). Cu(Im)$_2$ is a minor species (less than 10% of a total Cu(II) complexation anywhere) and therefore hardly distinguishable in the UV-Vis spectra. CuHL and CuL are both 3N + H_2O complexes, differing by protonation of the AHH C-terminus. Both produce the *d-d* band around 600 nm. Upon the further pH increase, Im starts replacing the equatorial water molecule in the 3N complex resulting in a formation of ternary Cu(L)(Im) complex with λ$_{max}$ at about 560 nm, and maximal appearances at pH 6.7. The ternary complex is also clearly distinguishable *via* CD spectroscopy, being blue-shifted from the parent complex by 50 nm. Cu(AHH)(Im), a 3N+N^{Im} complex possesses a 3N core as indicated by the CD spectral pattern (a single maximum in a d-d region rather than an intensive negative band of a 4N complex). Further increase of pH above 6.7 causes a formation of a small amount of CuH$_{-1}$L (about 20%). Above pH 8.3 the band shifts towards 512 nm which is consistent with potentiometric data and a formation of CuH$_{-2}$L (a 4N species with deprotonated His, see Table 1 for details).
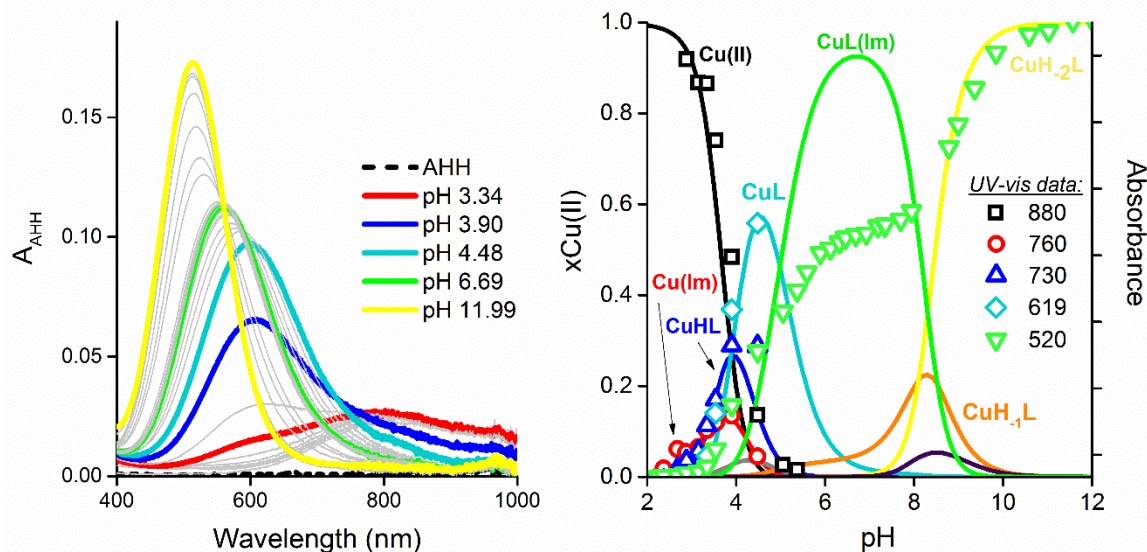
Figure 3: a) The pH titration of Cu(AHH) with 50 mM Im followed by UV-Vis. Experimental conditions: 1.8 mM CuCl$_2$, 2 mM AHH, titrated with aliquots of NaOH. b) Species distribution diagram for AHH/Cu(II)/Im complexes at 25 °C calculated using potentiometric stability constants for 1.8 mM CuCl$_2$, 2 mM AHH, and 50 mM Im (as used in UV-vis titration). The left-side axis denotes molar fractions of Cu(II) complexes. L stands for AHH. Calculated species are marked with solid lines. Data points correspond to the absorbance at wavelengths showcasing the formation of specific Cu(II) species.

Table 1. Protonation constants for AHH and Im and stability constants for their Cu(II) complexes, determined by potentiometry at 25 °C and I = 0.1 M. Previously reported constants for AHH and Cu(AHH) shown for comparison.[15]

	Species	Logβ ±SD	pK	Coordination mode/ deprotonation event
Protonation constants used for model calculations				
Im	LH	7.08 ± 0.003		
AHH	LH	8.18	8.18	N-term
	LH$_2$	15.22	7.05	His
	LH$_3$	21.32	6.10	His
	LH$_4$	23.57	2.20	C-term
Stability constants of binary complexes				
Im/Cu	Cu(Im)	4.16±0.04		
	Cu(Im)$_2$	7.96 ±0.06		
AHH/Cu	CuHL	16.54	n.a.	**3N:** N^{NH2}, N$^-$, N$^\pi$, protonated COOH
	CuL	12.66	3.88	**3N:** N^{NH2}, N$^-$, N$^\pi$, COO$^-$
	CuH$_{-1}$L	6.23	6.43	**4N:** N^{NH2}, 2N$^-$, N$^\pi$, COO$^-$, protonated His
	CuH$_{-2}$L	-1.87	8.09	**4N:** N^{NH2}, 2N$^-$, N$^\pi$, COO$^-$, deprotonated His
	CuH$_{-1}$L$_2$	9.81	n.a.	**3N+N$^\pi$:** N^{NH2}, N$^-$, N$^\pi$ and N$^\pi$
Stability constant of ternary complex				
AHH/Cu/Im	CuL(Im)	16.07 ± 0.1*		**3N+N^{Im}:** N^{NH2}, N$^-$, N$^\pi$ and N^{Im}

*- See SI for details of calculations

The data in Fig. 3 and Fig. S4 are fully consistent with the formation of the 3N + N^{Im} ternary complex in the presence of 50 mM Im at pH 5-10. Its absolute stability constant calculated consistently from potentiometry and UV-Vis and CD titrations is 2200±80 M^{-1}, 20 times higher than the apparent binding at pH 7.4. The 3N+N^{Im} complex can become more stable in comparison to the 4N complex depending on the pH value and the Im concentration while at pH 7.4, 8.02 mM Im is required to yield 50% of the 3N+N^{Im} versus the 4N complex.

To see if this interaction could be extrapolated to other external nitrogen bearing ligands, we explored the effect of azide, which binding to Cu(II) generates a very characteristic and well defined ligand to metal charge transfer (LMCT) band in the absorption spectrum at ~350 nm.[24] Thus, it was possible to monitor the shift of the *d-d* band of Cu(AHH) and the formation of the azide LMCT band simultaneously (Fig. S5 and S6). Indeed, formation of LMCT and shift of d-d bands occurred in parallel upon azide titration. Limitation of solubility of azide in the stock solution restricted the titration range to 100 mM. The LMCT band increase was not fully saturated at 100 mM. Similarly, the *d-d* band shifted from 525 nm to 600 nm, but this shift was not complete. Since the plateau was not reached no accurate $^cK_{7.4}$ could be determined. This result indicates that azide, like Im, is able to switch the coordination of Cu(AHH) from 4N to 3N + N_3^- at pH 7.4 by binding at the equatorial site, although much less efficiently.

The present work shows that the Cu(II) coordination to the peptide AHH can be easily changed by an external chemical stimulus. The stimulus is a Cu(II) ligand, able to bind in a mono-dentate manner to Cu(II) and hence shift the equilibrium from 4N for to 3N + N mode. This enlarges the scope of the shift induced by pH as reported in the past.[15,18] The different species have characteristic spectroscopic features. The 3N + N absorption depends on the identity of the external ligand, so the complexes 4N, 3N + N^{Im}, 3N + N_3^-, and 3N + H_2O all show different UV-Vis, CD and EPR signatures and have different apparent affinities (Cu(AHH)/Azide: 24 M^{-1}, Cu(AHH)/Im: 111 M^{-1}). They can be distinguished by naked eye in a concentrated solution (mM). Moreover, the relative Cu(II)-binding strength of a monodentate ligand can be easily followed by the shift of the *d-d* band. This might be of interest for sensing of small Cu(II) binding molecules. The impact of an external chemical ligand is not restricted to AHH, but it is also possible for the more general motif XHH, as the side chain of the 1st amino acid is not directly involved in Cu(II)-coordination (Scheme 1). However, the identity of X can certainly have an impact on the efficiency in shifting the equilibrium by secondary coordination sphere effects. We are aware of several such XHH sequences in human proteins/peptides, of which two were demonstrated to form very high affinity 4N complexes ($^cK_{7.4} > 10^{14}$ M^{-1}): endostatin (SHH-) and amyloid-β12-x (VHH-), one of the prominent products of enzymatic amyloid-β degradation.[25–27] Coordination properties of these hybrid ATCUN with biologically relevant N ligands (His for instance) warrant further investigations.

Notes and references

1   C. Harford and B. Sarkar, Acc. Chem. Res., 1997, 30, 123–130.

2   J. R. Turnlund, Am. J. Clin. Nutr., 1998, 67, 960S–964S.

3   D. G. Barceloux and D. Barceloux, J. Toxicol. Clin. Toxicol., 1999, 37, 217–230.

4   K. Jomova and M. Valko, Toxicology, 2011, 283, 65–87.

5   M. C. Linder, Metallomics, 2016, 8, 887–905.

6   E. I. Solomon, D. E. Heppner, E. M. Johnston, J. W. Ginsbach, J. Cirera, M. Qayyum, M. T. Kieber-Emmons, C. H. Kjaergaard, R. G. Hadt and L. Tian, Chem. Rev., 2014, 114, 3659–3853.

7   P. Gonzalez, K. Bossak, E. Stefaniak, C. Hureau, L. Raibaut, W. Bal and P. Faller, Chem. - A Eur. J., 2018, 24, 8029–8041.

8   L. Pickart and A. Margolina, Int. J. Mol. Sci., 2018, 1987.

9   L. D. Pettit, S. Pyburn, W. Bal, H. Kozlowski, M. Bataille and H. Kozlowski, J. Chem. Soc. Dalt. Trans.,

1990, 240, 3565.

10   H. Kozłowski, W. Bal, M. Dyba and T. Kowalik-Jankowska, Coord. Chem. Rev., 1999, 184, 319–346.

11   C. Hureau, H. Eury, R. Guillot, C. Bijani, S. Sayen, P.-L. Solari, E. Guillon, P. Faller and P. Dorlet, Chem. - A Eur. J., 2011, 17, 10151–10160.

12   K. Bossak, M. Mital, J. Poznański, A. Bonna, S. Drew and W. Bal, Inorg. Chem., 2016, 55, 7829–7831.

13   H. Sigel and R. B. Martin, Chem. Rev., 1982, 82, 385–426.

14   S. Mena, A. Mirats, A. B. Caballero, G. Guirado, L. A. Barrios, S. J. Teat, L. Rodriguez-Santiago, M. Sodupe and P. Gamez, Chem. - A Eur. J., 2018, 24, 5153–5162.

15   P. Gonzalez, B. Vileno, K. Bossak, Y. El Khoury, P. Hellwig, W. Bal, C. Hureau and P. Faller, Inorg. Chem., 2017, 56, 14870–14879.

16   C. N. Beuning, B. Mestre-Voegtlé, P. Faller, C. Hureau and D. C. D. C. Crans, Inorg. Chem., 2018, 57, 4791–4794.

17   A. Trapaidze, C. Hureau, W. Bal, M. Winterhalter and P. Faller, J. Biol. Inorg. Chem., 2012, 17, 37–47.

18   G. E. Jackson, A. N. Hammouda, F. M. Elmagbari and R. P. Bonomo, Polyhedron, 2017, 123, 23–32.

19   R. Kotuniak, T. Fraczyk, P. Skrobecki, D. Płonka and W. Bal, Inorg. Chem., 2018, 57, 15507–15516.

20   R. Meng, J. Becker, F. T. Lin, S. Saxena and S. G. Weber, Inorganica Chim. Acta, 2005, 358, 2933–2942.

21   S. Pizzanelli, C. Forte, C. Pinzino, A. Magrì and D. La Mendola, Phys. Chem. Chem. Phys., 2016, 18, 3982–3994.

22   S. J. Lau and B. Sarkar, Biochem. J., 1981, 199, 649–56.

23   W. E. Antholine, D. H. Petering and L. Pickart, J. Inorg. Biochem., 1989, 35, 215–224.

24   L. Casella, M. Gullotti, G. Pallanza and M. Buga, Biol Met., 1990, 3, 137–140.

25   A. Kolozsi, A. Jancsó, N. V Nagy and T. Gajda, J. Inorg. Biochem., 2009, 103, 940–947.

26   M. Mital, W. Bal, T. Frączyk, S.C. Drew, Inorg. Chem, 2018, 57, 6193-619700391.

27   K. Bossak-Ahmad, M. Mital, D. Płonka, S.C. Drew, W. Bal, Inorg. Chem. 2019, 58, 932-943